A statistical model for variability of the Arctic Ocean surface layer salinity

Ekaterina Chernyavskaya[1], and Ivan Sudakov[2,3*]

[1]Department of Oceanography, Arctic and Antarctic Research Institute, Bering str. 38, St. Petersburg, 199397 Russia.

[2]Department of Mathematics, University of Utah, 155 S 1400 E, Room 233, Salt Lake City, UT 84112-0090 USA.

[3]Department of Informatics, Novgorod State University, B. St.-Peterburgskaya str. 41, Veliky Novgorod, 173003 Russia.

* corresponding author:

email: sudakov@math.utah.edu

Abstract

Significant salinity anomalies were observed in the Arctic Ocean surface layer during the last decade. On the base of gridded data of winter salinity of the upper 50 m layer for the period 1950-1993 and 2007-2012 we investigated the features of the interannual variability of salinity fields, tried to identify the causes of its anomalies, and develop a statistical model for the prediction of surface layer salinity fields. The Statistical model based on linear regression equations linking the principal components with environmental factors such as atmospheric circulation, river runoff, ice processes, and water exchange with neighboring oceans. Using this model, we obtained prognostic fields of the Arctic Ocean surface layer salinity for the winter period 2013-2014. Prognostic fields demonstrate the same tendencies of the surface layer freshening that were observed before.

Key words: Arctic Basin, surface layer, salinity anomalies, empirical orthogonal functions, clusters analysis.

Introduction

The Arctic Ocean is very sensitive to changing environmental conditions. Its surface layer is a key component of the Arctic climate system, which constitutes the dynamic and thermodynamic links between the atmosphere and the underlying waters (Carmack 2000). The stability and development of the ice cover are associated with mixed layer thickness, upper layer salinity, and upper halocline, which state the geographic distribution of sea ice and variability. In this context, the Arctic Ocean surface layer is a reliable indicator of climate change in the Arctic (Zaharov 1996).

Thermohaline structure of the Arctic Ocean surface layer has also undergone significant changes in recent years (Figure 1). Of particular interest is the great freshening of the Canada Basin surface layer that has not been observed in this region since 1950 (Timokhov et al. 2011) until the early 1990s. However, in (Jackson et al. 2012) has emphasized that the processes related to warming and freshening of the surface layer in this region have transformed the water mass structure of the upper 100 m.

In addition, there are observations of significant salinification of the upper Eurasian Basin that began around 1989. One hypothesis for this is the increasing of Arctic atmospheric cyclone activity in the 1990s that led to a spectacular changing of the salinity in the Eurasian Basin. This can be explained through two mechanisms of salinization: 1) changes in the rivers inflow, and 2) increased brine formation due to changes in Arctic sea ice formation. The high salinization in this region altered the formation of cold halocline waters, weakened vertical stratification, and released heat upward from below the cold halocline layer (Johnson & Polyakov 2001). The other reason of salinification is influence of the Atlantic waters (AW), which by 2007 became warmer by about 0.24˚C then in the 1990s. Observations show that increase in the Arctic Ocean salinity has accompanied the warming. This led to significant shoaling of the upper AW boundary (up to 75-90 m in comparison with climatic values) and weakening of the upper-ocean stratification in the Eurasian Basin as well (Polyakov et al. 2010). However, current observations also show that the upper ocean of the Eurasian Basin was appreciably fresher in 2010 than it was in 2007 and 2008 (Timmermans et al. 2011).

It (Zhang et al., 2003) has been emphasized that the fresh water balance and salinification of the Arctic Ocean are key players in the mixed layer. In turn, it is well known that the crucial factors of the surface water mass transformation are advection of the salinized ocean waters and influence of this process on the halocline and, on the other, the changes in the density field of the ocean conduct to the surface water and sea ice circulation.

Why salinity was chosen as the object of this investigation. It is known that for the Arctic Ocean, water density depends more on water salinity than on water temperature, and hence the thermohaline circulation is mainly determined by salinity distribution. This conclusion comes easily from an analysis of a linear equation for seawater state:

$$\rho = \rho_0 - \varepsilon T(T - T_0) + \varepsilon S(S - S_0), \qquad (1)$$

where ρ_0, T_0, S_0 are some initial values of water density, temperature, and salinity; $\varepsilon T = 7 \cdot 10^{-5}$ g/(cm^3·K), $\varepsilon S = 8 \cdot 10^{-4}$ g/(cm^3·‰).

Vertical variations of temperature and salinity in the upper layer can reach 0.5˚C and 1‰ respectively. Thus, if we put these numbers into an equation we can get the contributions of temperature and salinity in changes of water density, which are about 4 and 96 % respectively.

Transfer of the briny surface waters and ice from the Arctic Ocean to the North Atlantic is a significant component of the global ocean circulation. Thus, the investigation of the variability of the surface layer can make a great contribution to understanding the climate-ocean feedbacks. Particularly, abrupt changes in the surface layer salinity may lead to a tipping point in the global ocean circulation (Lenton et al., 2009). In (Lenton, 2011) was defined that the climate 'tipping point' may happen if a small change in forcing triggers a strongly nonlinear changes of the internal properties of the system, that can lead to changing its future states. We may interpret a “forcing triggers” as anomaly in interannual salinity variability. Anyway, the robust mathematical models are required for implementation of this hypothesis. In present time we have a lot of different physical models of the surface layer salinity For example, the sea ice salinity models can model significant changes in physical macroscopic properties as well as microscopic properties such as the distribution of brine channels (Vancoppenolle, et al, 2009b). Besides that, to use the regional climate models (for specific seas) for understanding of scale variation is not an appropriate approach.

Thus, changes in salinification of the Arctic Ocean are one of the key players in the Arctic climate system, which connects this system to the global climate system. This curious system leads us to a better understanding of feedbacks, tipping points, and anomalies.

We propose to develop our model expressed by the ideas of L. Timokhov (Timokhov et al., 2012). This statistical model of variability, of the Arctic Ocean winter salinity, in the 5–50 m layer is used the method of reconstruction of the winter fields of salinity which have been suggested in (Pokrovsky & Timokhov 2002). This study is devoted to the development of a statistical model of variability of the Arctic Ocean winter salinity in the 5–50 m layer. The model is based on equations of multiple correlations for the time series (principal components, PC) associated with the first five leading modes of the Empirical Orthogonal Function (EOF) analysis applied to the salinity fields. The contribution of atmospheric factors, hydrological processes and pre-history of spatial distribution of salinity can be interpreted through determining of the structure of the multiple correlation equations.

Based on gridded data of winter salinity of the upper 50 m layer for the periods of 1950-1993 and 2007-2012, we investigated the features of the inter-annual variability of salinity fields, tried to identify the causes of its anomalies, and made a statistical model for the prediction of surface layer salinity fields.

Cluster analysis of the surface salinity allowed identifying 6 types of spatial distribution of the salinity fields, which differ from each other by position of the fresh water core, position of the Transpolar Drift frontal zone, and value of horizontal salinity gradient. It has been shown that the structure of salinity fields (of 1990-1993 and 2007-2012) greatly differs from previous years. Uniqueness of halin structure (during 2007-2012) was also confirmed by the results of the decomposition of the surface salinity fields on Empirical Orthogonal Functions.

Analysis of the equations for the first five PCs showed that surface salinity fields were influenced mostly by atmospheric processes. Moreover, the structure of the salinity fields due to their conservatism can save and accumulate the after-effects of atmospheric processes occurring up to 2-3 years ago (according to the results of the correlation analysis of the links between PCs and various external factors).

We obtained using the PCs, calculated by the model, forecast fields of the Arctic Ocean surface layer salinity for the winter period 2013-2014. Prognostic fields demonstrate the same tendencies of the surface layer freshening that were observed before.

2. Data Set and Method

2.1. Data Set

This study is based on the collection of more than 6,419 instantaneous temperature and salinity profiles with data available at the standard levels (5,10, 25, 50, 75, 100, 150, 200, 250, 300, 400, 500, 750, 1000 and so on every 500 meters) collected between 1950-1993 and obtained from the Russian Arctic and Antarctic Research Institute (AARI) database; this is complemented by data made available between 2007-2012 from the expeditions of IPY and after, which consisted of CTD and XCTD data originating from ITP-buoys. The average vertical resolution of these profiles were 1 m. The first database was introduced by Lebedev et al. (2008). In areas where observations were missing, temperature and salinity data were reconstructed in a regular grid for the period of 1950 to 1989. Also, some data was found in the joint U.S. Russian Atlas of the Arctic Ocean for winter (Timokhov & Tanis 1997). Thus the working database is represented by grids with spatial resolution of 200 per 200 km, covering a deep part of the Arctic Ocean (with depth more than 200 m).

According to researchers (Treshnikov 1959; Rudels et al. 1996, 2004) the average thickness of the Arctic Ocean mixed layer for the winter season is 50 m. Termohaline characteristics of the surface layer fully reflect the effects of atmospheric and ice processes, as water most directly exposed to the atmosphere and ice lies within the mixed layer (Sprintall & Cronin 2001).

For data analysis, we also used different factors such as river runoff (Joint US-Russian Atlas of the Arctic Ocean 1997; http://rims.unh.edu/data/station/list.cgi?col=4), the area of the ice-free surface in the Arctic seas in September (http://www.aari.ru/projects/ECIMO/index.php?im=100), the ice extent in the Arctic Ocean (http://www.esrl.noaa.gov/psd/data/gridded/tables/arctic.html), and some indexes of atmospheric circulation. We found AO, NAO, and PNA indexes were at http://www.cpc.ncep.noaa.gov/; AMO indexes at http://www.esrl.noaa.gov/psd/data/timeseries/AMO/); and PDO data downloaded from http://jisao.washington.edu/pdo/. Average monthly AD indexes can be found at http://www.jisao.washington.edu/analyses0302/.

2.2. The statistical method

In this section, we shortly describe the statistical model for analyzing the fields of oceanographic records, which was introduced in (Pokrovsky & Timokhov 2002), that was used to obtain gridded salinity fields

$$\begin{gathered} z_i = z_i^{(r)} + e,\ \langle z_i z_j \rangle = \sigma_{x_i x_j},\ \langle z_i e_i \rangle = 0, \\ \langle e_i \rangle = 0, \langle e_i e_j \rangle = \delta_{ij}\sigma_e^2 = \sigma_{e_{ij}}^2 \end{gathered} \tag{2}$$

We assume that $z(t, x)$ – measured value of an oceanographic record (e.g. temperature or salinity) is a random function of time t and coordinates x. We can reproduce observed value of $z(t, x)$ as a sum of a true value $z^{(r)}(t, x)$ of the oceanographic record and an observational error $e(t, x)$. We also suppose that $z_i^{(r)}$ has spatial correlations to the records; a systematic error is not identified; a standard deviation of error does exist.

Biorthogonal decomposition of the oceanographic record can help to identify the connection between spatial and temporal distribution of the oceanographic record:

$$z(t_j, x_i) = \sum_k c_k^j f_k(x_i) + e(t_j, x_i), \tag{3}$$

where $f_k(x_i)$ – spatial empirical orthogonal function (EOF); c_k^j – calculated coefficient, so-called ***k*-th** principal component.

As the next step let's approximate EOF through linear combination of convenient analytical functions $P_l(x_i)$. Thus, the modified biorthogonal decomposition can be written

$$z(t_j, x_i) = \sum_k d_l^j P_l(x_i) + e(t_j, x_i), \tag{4}$$

here $d_l^j = \sum b_{kl} c_k^j$.

The main goal of this spectral analysis method is to estimate coefficients of spectral decomposition $C = \left|c_k^j\right|$ and $B = \{b_{kl}\}$. Actually, this approach is a combination between singular value decomposition and statistical regularization. These coefficients (modes) can be marked through the real physical processes which influence salinity (see the physical model below).

2.3. Statistical model

Next, we will describe the approaches to data analysis which were used for physical interpretation of our statistical model.

Researchers (Polyakov et al. 2010; Rabe et al. 2011; Morison et al. 2012) have emphasized that the thermohaline structure of the surface layer has undergone significant changes over the last decade. However, we still don't understand the physical processes which led to these changes or what might be the future trends.

On the other side, we can assume that the analysis of variability of the surface layer (including salinity fields) of the Arctic Ocean may be based on the decomposition of empirical orthogonal function. This approach is useful in our case because decomposition on EOF gives modes and principal components (PC) which allow us to divide the variability in researched parameters on the spatial and temporal components. Each mode describes a certain fraction of a dispersion of the initial data. This fraction is inversely proportional to the order of a mode (Hannachi et al. 2007). The first 3-5 modes describe most of the dispersion of the analyzed salinity fields, which allow significantly compressing the information contained in the original data (Hannachi et al. 2007; Borzelli & Ligi 1998). EOF decomposition was carried out for the average salinity fields for the layer 5-50 m as well as obtained time series of PCs for the periods of 1950-1993 and 2007-2011.

We applied our statistical model to interpret the physical processes through PCs. We approximate the time series of principal components to identify predictors that determine variability of the salinity fields; also, it helps to obtain the equations for projection of future changes. The statistical model is presented by a system of linear regression equations constructed for the first five PCs, as the first five EOF yields above 77 % of the total variance of the salinity data. The principal components were associated with these factors: the atmospheric circulation indexes (AMO, AO, NAO, PDO, PNA, AD), water exchange with Pacific and Atlantic Oceans, river runoff, and the area of the ice-free surface in the Arctic seas in September. Firstly, these indexes were introduced in the work of Pokrovsky and Timokhov (2002). In table 2 you can find physical interpretation of these indexes. We should note that we did introduce one assumption, that time series of the Arctic and Atlantic oceans water exchange can be presented through AMO indexes.

2.4. Cluster analysis

We use cluster analysis with the aim to systematize the existing data. You can find a detailed description of cluster analysis in the work of Ward (1963). According to this approach, we represent the salinity filed as a grid with nodes. Each of these nodes contains information about salinity in the region, and the measure of the distance between two nodes was introduced through a Euclidean metric:

$$D_{ij} = (\sum_{ij} (S_i - S_j)^2)^{\frac{1}{2}} \quad (5)$$

here S_i и S_j - value of salinity in a node for the different time.

Consequently, this analysis allows us to obtain the hierarchical salinity fields with a feature of statistical identity (Fig.2). The figure shows that the salinity fields have structural differences and thus are grouped in clusters for consecutive years. Based on the tree ties, we have identified six of the largest groups in temporal scale as well as six of the basic types of salinity fields. The first cluster reproduces the field for the following years - 1950-59, 1976-77 and 1989; the second cluster includes 1960-1965; the third cluster includes 1966-1975; the fourth cluster includes 1981-1988; the fifth cluster includes 1978-1980; and the sixth cluster includes 1990-93 and 2007-2012 .

In this paper, cluster analysis was completed for the data series of an average salinity at a depth of 5-25 m for the period of 1950-1989. Similar results were obtained using other methods of cluster analysis (e.g., complete linkage, weighted pair-group average). This shows that the chosen division into clusters is stable and proper. In addition, similar dendrograms were found in the work of Koltyshev et al. (2008). It also confirms the robustness of our classification. Within the framework of our classification the field type may persist for two to nine years.

We calculated the average salinity fields for each period of each group. It allows us to find the differences (from cluster to cluster) in the structure of salinity fields (Fig.3).

Cluster 1: Our analysis for these years shows that a desalination zone occupies the southern part of the Canada Basin (Fig. 3a). The salt-frontal zone lies along the Lomonosov Ridge. This kind of distribution of salinity fields is formed under the dominance of a cyclonic mode of the atmospheric circulation (Proshutinsky & Johnson 1997).

Cluster 2: Here the distribution of salinity fields mostly look like a freshening zone with multiple cores, which extends from the Beaufort Sea to the North Pole (Fig. 3b). This structure of the spatial distribution of salinity is formed because of the anticyclonic mode of the atmospheric circulation at the different positions of the anticyclonic core.

Cluster 3: The main feature of the salinity distribution here is an extensive area of freshening which occupies the entire Canada Basin. As a result of that, the salinity frontal zone is shifted to the region of the Gakkel Ridge (Fig. 3c). This structure of the salinity spatial distribution is formed at the anticyclonic mode of the atmospheric circulation.

Cluster 4: We can see here that this cluster combines the salinity fields with a tendency to the formation of several zones in the prefrontal area of desalination, which is moving into the area of the Gakkel Ridge (Fig. 3d).

Cluster 5: Here the core of freshening has a displacement to the region of the Makarov basin to the Northeast from the slope of the Laptev Sea shelf. Freshening zone extends from West to East (Fig. 3e).

Cluster 6: The zone of maximum freshening locates near to the center of the Canada Basin. Also, this zone is connected to the freshening zone in the Beaufort Sea. Additionally, we can see the formation of a small core of freshening close to the region which is North of the East Siberian Sea. The salt-frontal zone occupies the extreme Eastern position, lying on the Makarov Basin (Fig. 3f). This kind of salinity distribution is formed mainly under influence of highly developed cyclonic atmospheric circulation.

In addition, we can note, that cluster 6 is a separate branch with the largest Euclidean distance on the dendrogram. Thereby, since 1990 the structure of the salinity fields is undergoing significant changes, which were most pronounced in 2007-2012. These years can be isolated in a separate subbranch.

If we compare the variability of salinity in the Eurasian and Canada basins, we may conclude that the main difference in salinity fields for 2007-2012 (included in cluster 6) is in the amount of salinity of the Canada basin. During this period it was less than 0.8 ‰ comparing with average values. This means there has been a significant freshening of the surface layer, which has not been observed previously in more than 50 years of observation (Fig. 1).

2.5. Decomposition of surface salinity fields on EOF

As a result of EOF decomposition of the average salinity fields for 5-50 m layer, we obtained two sets of modes and principal components for the period of 1950-1993 years (series 1), and for the same period by adding the 2007-2011 years (series 2). In summary, the first three modes obtained by decomposition of series 1 describe over 60% of the total dispersion of the initial fields; additionally, the first three modes of series 2 describe almost 67.5% of the total dispersion. These modes for both decompositions are significantly different.

We can see that the first mode has an additional core in the Canada Basin; we observed reorientation of the cores for the rest of the modes (Fig. 4). The first mode of series 1 describe 38% of the total salinity variability, and the first mode of series 2 takes into account 51.5% of the initial data dispersion. The first mode is associated with the influence of large-scale atmospheric circulation in the Arctic (Timokhov et al. 2012). Therefore, we can conclude that the role of atmospheric circulation in the formation of the surface salinity fields in the Arctic Basin has grown significantly over the last decade. Thus, the modes obtained by decomposition in series 1 cannot take into account the essential features of the distribution of surface salinity fields associated with the freshening waters of the Canada Basin. Therefore, for further analysis we will use the principal components and modes obtained upon decomposition of series 2.

Figure 5 illustrates the differences between clusters allocated previously for classification of surface field salinity in terms of PCs. Clusters 1 and 6 are characterized by negative values of the three principal components; the difference between the clusters is in the amount of values of the principal component 1 (PC_1). Clusters 3, 4, and 5 are characterized by dominant positive values PC_1 and different sign and magnitude of PC_2 and PC_3. Cluster 5 is the opposite of cluster 6 in terms of PC values. As we see from Fig.3 (e, f), a shift in the signs of the principal components can be explained by moving the core of freshening from the Makarov Basin to the Beaufort Sea, and the degree of freshening appeared to determine the absolute value of PC_1.

In the late 80s, the atmospheric circulation regime began to change (Steele & Boyd 1998; Kuražov et. al 2007; Proshutinsky et al. 2009; Morison et al. 2012). Degradation of the Arctic anticyclone is the great example of this changing. Some changes in the structure of the surface pressure field were observed. This happened because of a frequent recurrence of large values of the AD indexes.

According to Wang et al. (2009) this could be a reason for local minima of sea ice in the summers of 1995, 1999, 2002, 2005 and 2007. In addition, in the late 80s inflow of warm and saline Atlantic water into the Arctic basin increased (Frolov 2009). At the beginning of this century, heat flow of Pacific waters through the Bering Strait to the Chukchi Sea increased (Woodgate et al. 2010).

We calculate a correlation of the principal components with different climate processes such as the atmospheric processes, river runoff, and volume of water coming in through the straits of the Arctic Basin (Table 1). Statistically significant coefficients were obtained for factors reflecting influences on the processes listed above. Thus, we can assume that Cluster 6 of the dendogram is the consequence of these processes.

The time series of some of these processes have been normalized over the interval 0 to 1. We chose the clusters (1950-59, 1976-77, 1989 (cluster 1) and 1990-1993, 2007-2012 (cluster 6)) with a similar structure of their surface salinity fields (Fig. 3a and 3f), but with different values of salinity in the water cycle of the Beaufort Sea. The histogram (Fig. 6) shows that the relative values of almost all factors for the years 1990-1993 and 2007-2012 were significantly higher than in the year 1950. Temperature anomalies, the area of ice-free regions of the shelf seas, winter and summer AO indexes and DA indexes have reached the highest values.

2.6. The linear regression equation for the principal components

A set of external factors having the most correlation coefficients with the main components of salinity decomposition (Table 1) has been defined based on the results of correlation analysis. As a result of the approximation we obtained the following equations for the first five principal components:

$$PC_1=-0.96\times AO_{I\text{-}IV}(-2)-1.11\times AO_{I\text{-}IV}(-1)-1.62\times NAO_{XII\text{-}IV}(-1)-3.17\times AMO(-8)-7.38\times BS(-3)-0.01\times RIV_{EC}(-3)+0.003\times RIV_{KL}(-5)-0.003\times OW_{KLEC}(-1)+9.53 \quad (6)$$

$$PC_2=-0.57\times AO_{I\text{-}IV}(-1)-1.49\times AO_{VII\text{-}IX}(-1)+6.76\times AMO(-10)+0.88\times PDO(-3)-0.71\times PDO(-10)-3.09\times BS(-4)-0.006\times RIV_{LE}(-3)-0.005\times RIV_{EC}(-5)+0.003\times OW_{KLEC}(-1)+6 \quad (7)$$

$$PC_3=-0.68\times NAO_{XII\text{-}IV}(-3)+7.65\times AMO(-5)-3.53\times AMO(-8)-2.42\times AMO(-9)+3.42\times AMO(-11)+1.40\times PDO(-10)+6.44\times Tair_{II\text{-}IV}(-1)-5.80\times BS(-3)+0.002\times RIV_{KLEC}(-3)-0.002\times RIV_{KLE}(-5)-0.006\times RIV_{LE}(-6)-0.001\times OW_{KLEC}(-1)+13 \quad (8)$$

$$PC_4=0.78\times NAO_{XII\text{-}IV}(-1)+0.59\times PNA_{X\text{-}IV}(-1)-0.60\times PNA_{VII\text{-}IX}(-1)+2.79\times AMO(-6)-2.18\times AMO(-12)-0.66\times PDO(-6)-8.27\times BS(-4)-0.006\times RIV_{LEC}(-6)+0.001\times OW_{KLEC}(-1)+0.002\times OW_{EC}(-1)+8.83 \quad (9)$$

$$PC_5=-0.68\times NAO_{I\text{-}IV}(-1)-2.38\times AMO(-7)-3.52\times AMO(-12)+4.72\times Tair_{II\text{-}IV}(-2)+0.001\times IceExt(-1)-0.002\times RIV_{KL}(-5)+0.007\times RIV_{LEC}(-6)+0.001\times OW_{KLEC}(-2)-11.74 \quad (10)$$

Where AO, NAO, PNA, AMO, PDO – atmospheric indices, and the lower case indicates the months of an average period; RIV – sum of annual river runoff for the arctic seas, and the lower case indicates the first letters of the sea name (K–Kara Sea, L–Laptev Sea, E–East-Siberian Sea, C–Chukchi Sea); BS – inflow through the Bering Strait; OW – sum area of open water in the arctic seas in September, and the lower case indicates the first letters of sea name; IceExt − area of ice extent in the Arctic Ocean in September; Tair – air temperature anomalies in the Arctic, and the lower case indicates months of an average period.

Each equation includes a set of predictors that simulate both effects of atmospheric and hydrological processes. In this case, hydrological processes have dominant influence on PC_1 (in a ratio of 60/40%) and, vice versa, atmospheric processes are the major factor influencing on PC_2 and PC_3 in the same proportion. Atmospheric and hydrological processes make approximately the same contribution (in the ratio of 47/53%) to the formation of the interannual variability of PC_4.

Discussion and Summary

We presented here a statistical model of inter annual variability of the Arctic Ocean surface layer salinity. This research builds on already established approaches used by Pokroivsky and Timokhov (2002) (specifically, their reconstruction of salinity fields applying modified EOF methods).

However, first time, our contribution to their work is the formulation of an uniform statistical model, which can be used like a universal tool for analysis of inter annual variability of Arctic Ocean surface layer salinity. Moreover, we suggested some additional things to improve the ideas presented in previous research. For example, as opposed to this research, we do not take into account the previous values of the principal components (history) that simplifies the calculations and allows to increase the earliness. In addition, we also make calculations using the current observational data, which is quite important for understanding the physical processes during dramatic current changes in the Arctic sea ice.

Equations (4) - (8) describe the first five principal components for the period 1950-2014; PCs for 1950-2011 obtained from these equations, have a good agreement with the values of PCs directly derived from the decomposition of salinity fields on EOF (Fig. 7). Salinity fields for 1994-2006 can be reconstructed with the help of this model. We noted above that this period has the gaps in observational data.

We make these conclusions because, as we mentioned in the verification, this model cannot reproduce exact principle components for the short-term time series, although the trends in variability of all five PC are reproduced correctly. Therefore, the model can be used for tracking long-term processes of the structure transformation of salinity fields. Using this useful tool we can make projections for anomalies, its frequency, and ultimately to approach an understanding of these sophisticated physical processes.

Validation of the model was determined by calculating an error of reconstruction of surface salinity fields. The difference between the real and reconstructed salinity fields is determined as a percentage by the following formula:

$$Inc = (\sigma(S_f - S_c)/\sigma(S_f))\cdot 100\%, \tag{11}$$

where σ – standard deviation; S_f – actual salinity; S_c – calculated salinity.

The error in the reconstruction of salinity fields is 25.2 % (Fig. 8). The reasons for this may be several:

1. The first five EOF modes describe more than 77 % of the variability of the initial fields. It is possible that the characteristics of salinity fields may reproduce the higher order modes (Borzelli & Ligi 1998). If the order of a mode increases, then the dispersion decreases. So, it can enhance uncertainty in interpreting the physical processes associated to PCs. Thus, the error of reconstruction in salinity fields, initially incorporated to the model, is about 23%.

2. Equations (6)-(10) were obtained for the continuous data series for 1950-1993. However, we applied these equations to short-term and independent data series for 2007-2011. Of course, it is not enough for a statistically significant assessment of the quality of PCs modeling during this period. Nevertheless, the overall trend in PCs variability is reproduced correctly.

3. In the last decade, there are significant changes in the thermohaline state of the surface layer. It is quite possible that these critical transitions in this system (Timokhov et al. 2011) can influence the structure of PCs. We need to adapt this model to these conditions of uncertainty.

Also, we apply this model for the reconstruction of salinity fields for 2013-2014. It should be noted that the time series of some predictors were insufficient in length for getting values of PCs. Therefore extrapolation was made.

As a result, we obtained the salinity field, which corresponds to the observed trends in recent years. This has saved significant freshening in the Canada Basin as well as big spatial gradients between the Eurasian and Canada Basins. According to our projections for 2013-2014 (Fig. 9), freshened water from the Beaufort Gyre will move up westward along the Siberian continental slope. In 2014, the spatial structure of the salinity field is similar to the structure that is typical for fields belonging to cluster 4 (1981-1988), but they differ by the surface salinity values in the Beaufort Sea.

Acknowledgments

In preparing this text, we have benefited from discussions with L.A. Timokhov and Jessica R. Houf. We are grateful for the financial support from Otto Schmidt Laboratory for Polar and Marine Research (grant No. OSL-13-05) and from Russian Foundation for Basic Research (grant No. 14-01-31053 мол_а). IS acknowledges support from "Mathematics and Climate Research Network" (NSF-funded project, grant No. DMS-0940249) and from the Russian Federation President Grant (No. MK-128.2014.1). IS acknowledges the kind hospitality of the Isaac Newton Institute for Mathematical Sciences (Cambridge, UK) and of the Mathematics for the Fluid Earth 2013 programme, as well as the Dynasty Foundation for their support.

References:

Borzelli G. & Ligi R. 1998. Empirical Orthogonal Function Analysis of SST Image Series: a Physical Interpretation. *Journal of atmospheric and oceanic technology,* vol. 16, p. 682-690.

Carmack E.C. 2000: The Arctic Ocean's freshwater budget: sources, storage and export. In E.L. Lewis, E.P. Jones, P. Lemke, T.D. Prowse, P. Wadhams (eds.): *The Freshwater Budget of the Arctic Ocean.* Pp.91-126. Netherlands: Kluwer Academic Publishers.

Chernyavskaya E.A., Timokhov L.A. & Nikiforov E.G. 2013. Harakteristiki poverhnostnogo sloja i podstilajuščego ego haloklina Arctičeskogo bassejna v zimnij period (po dannym 1973-1979 gg). (Characteristics of the Arctic Ocean surface layer and underlying halocline in winter (according to the 1973-1979 period)). *Problemy Arktiki i Antarktiki* 1(95), p. 5-17.

Hannachi A., Jolliffe I.T. & Stephenson D.B. 2007. Empirical orthogonal functions and related techniques in atmospheric science: a review. *International Journal of Climatology* 27, 1119-1152.

Morison J. et al. 2012. Changing Arctic Ocean freshwater pathways. *Nature* 481, 66-70, doi 10.1038/nature10705

Overland J. E. & Wang M. 2007. Future regional sea ice declines. *Geophysical Research Letters 34*, L17705, doi 10.1029/2007GL030808.

Overland J. E., Wang M. & Salo S. 2008. The recent Arctic warm period. *Tellus* 60A, p.589-597.

Overland J.E. & Wang M. 2010. Large-scale atmospheric circulation changes are associated with the recent loss of Arctic sea ice. *Tellus* 62A, p.1-9.

Pokrovsky O.M. & Timokhov L.A. 2002. Rekonstrukcyja zimnih polej temperatury i solenosti Severnogo Ledovitogo okeana (The Reconstruction of the Winter Fields of the Water Temperature and Salinity in the Arctic Ocean). *Okeanologija,* vol.42, №6, p. 822-830.

Polykov I. V. et al. 2010. Arctic Ocean warming contributes to reduced Polar Ice Cap. *Journal of Physical Oceanography*, vol. 40, p. 2743-2756

Proshutinsky A.Y. & Johnson M.A. 1997. Two circulation regimes of the wind-driven Arctic Ocean. *Journal of Geophysical Research,* vol. 102, № C6, p. 12493-12514.

Proshutinsky A.Y. et al. 2009. Beaufort Gyre freshwater reservoir: State and variability from observations. *Journal of Geophysical Research,* vol. 114, doi 10.1029/2008JC005104

Rabe B. et al. 2011. An assessment of Arctic Ocean freshwater content changes from the 1990s to the 2006-2008 period. *Deep-Sea Research* 58, p. 173-185.

Rudels B., Anderson L.G. & Jones E.P. 1996. Formation and evolution of the surface mixed layer and halocline of the Arctic Ocean. *Journal of Geophysical Research*, vol. 101, №C4, p. 8807-8821.

Rudels B. et al. 2004. Atlantic sources of the Arctic Ocean surface and halocline waters. *Polar Research*, vol. 23, №4, p. 181-208.

Sprintall J. & Cronin M. F. 2001. Upper ocean vertical structure. *Encyclopedia of ocean sciences 6*, p. 3120-3129.

Steele M. & Boyd T. 1998. Retreat of the cold halocline layer in the Arctic Ocean. *Journal of Geophysical Research,* vol. 103, doi 10.1029/98JC00580

Stroeve J.et al. 2007. Arctic sea ice decline: Faster than forecast. *Geophysical Research Letters* 34, L09501, doi 10.1029/2007GL029703

Timmermans M.-L. et al. 2011. Surface freshening in the Arctic Ocean's Eurasian Basin: an apparent consequence of recent change in the wind-driven circulation. *European Geosciences Union General Assembly 2011. Austria, Vienna, 3-8 April 2011. Geophysical Research Abstracts 13*, EGU2011-5190.

Timokhov L. & Tanis F. (eds.) 1997. *Joint U.S.-Russian Atlas of the Arctic Ocean [CD-ROM]. Environmental Working Group*. Boulder, USA: University of Colorado.

Timokhov L.A. et al. 2011: Ėkctremal'nye izmenenija temperatury i solenosti vody arctičeskogo poverhnostnogo sloja v 2007-2009 gg. (The extreme changes of temperature and salinity in the Arctic Ocean surface layer in 2007-2009.) In I.Y. Frolov (ed.): *Okeanografija i morskoj led. (Oceanography and sea ice.)* Pp.118-137. Moscow: Paulsen.

Timokhov L.A.et al. 2012. Statističeskaja model' mežgodovoj izmenčivosti polej zimnej solenosti poverhnostnogo sloja. (Statistical model of interannual variability of the Arctic Ocean surface layer salinity in winter). *Problemy Arktiki i Antarktiki*, 1(91), p. 89-102.

Trešnikov A.F. 1959. Poverhnostnye vody v Arctičeskom bassejne. (Arctic Ocean surface waters.) *Problemy Arktiki* 7, p. 5-14.

Wang J. et al. 2009. Is the Dipole Anomaly a major driver to record lows in Arctic summer sea ice extent? *Geophysical Research Letters* 36, L05706, doi 10.1029/08GL036706

Ward J.H. 1963. Hierarchical Grouping to Optimize an Objective Function. Journal of the American Statistical Association 58, p. 236-244.

Woodgate R.A., Weingartner T. & Lindsay R. 2010. The 2007 Bering Strait oceanic heat flux and anomalous Arctic sea-ice retreat. *Geophysical Research Letters* 37, L01602, doi 10.1029/2009GL041621

Wu B., Wang J. & Walsh J.E. 2006. Dipole Anomaly in the Winter Arctic Atmosphere and Its Association with Sea Ice Motion. *Journal of Climate*, 19, p. 210–225.

Zaharov V.F. 1996. *Morskie l'dy v klimatičeskoj sisteme. (Sea ice in the climatic system)*. Saint-Petersburg: Hydrometeoizdat (Gidrometeoizdat).

Koltyšev A.E. et al. 2008. Krupnomasštabnaja izmenčivost' arealov rasprostranenija raspresnennyh vod v Arctičeskom bassejne. (Large-scale variability of areas of the Arctic Ocean fresh water distribution.). *Trudy AANII* 448, p. 37–58.

Lebedev N.V. et al. 2008. Specializirovannaja baza dannyh po temperature i solenosti vod Arktičeskogo bassejna i okrainnyh morej v zimnij period. (Specialized database for temperature and salinity of the Arctic Basin and marginal seas in winter.) *Trudy AANII* 448, p. 5-17.

Frolov I.E. et al. 2005. *Naučnye issledovanija v Arktike. (Scientific researches in Arctic.)* Vol. 1. Saint-Petersburg: Nauka.

Zhang, Xiangdong, Moto Ikeda, John E. Walsh, 2003: Arctic Sea Ice and Freshwater Changes Driven by the Atmospheric Leading Mode in a Coupled Sea Ice–Ocean Model. J. Climate, 16, 2159–2177. doi: http://dx.doi.org/10.1175/2758.1

T.M. Lenton, H. Held, E. Kriegler, J. W. Hall, W. Lucht, S. Rahmstorf, and H. J. Schellnhuber, Tipping elements in the Earth's climate system, Proceedings of the National Academy of Sciences 105 (2008), 1786-1793.

Lenton, T.M. (2011). Early warning of climate tipping points. Nature Climate Change, 1, 201-209.

Pokrovsky O.M., L.A. Timokhov., The reconstruction of the winter fields of the temperature and salinity in the Arctic ocean, Okeanologiya (Oceanology), 42(6), p. 822830.

Jackson, J. M., W. J. Williams, and E. C. Carmack (2012), Winter sea-ice melt in the Canada Basin, Arctic Ocean, Geophys. Res. Lett., 39, L03603, doi:10.1029/2011GL050219.

Vancoppenolle, M., T. Fichefet, and H. Goosse (2009b). Simulating the mass balance and salinity of Arctic and Antarctic sea ice. 2. Importance of sea ice salinity variations, Ocean Modelling, 27, 54-69

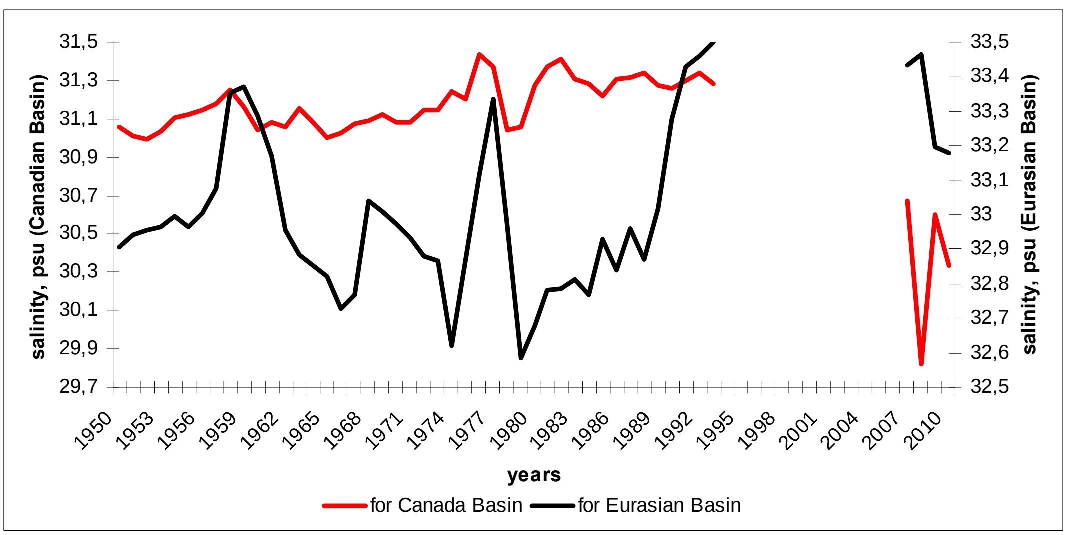

Fig. 1. Temporal changing in salinity on the depth 5-50 m (the Eurasian Basin and Canada Basin) is as an example of anomalies.

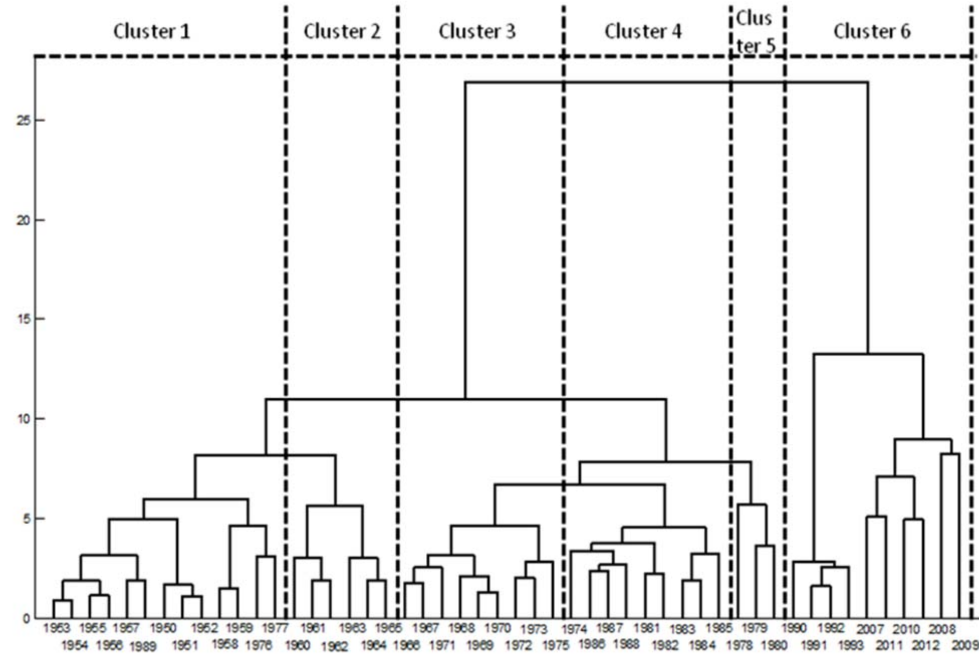

Fig. 2 Dendrogram of winter salinity fields for the layer 5-50 m in the Arctic basin.

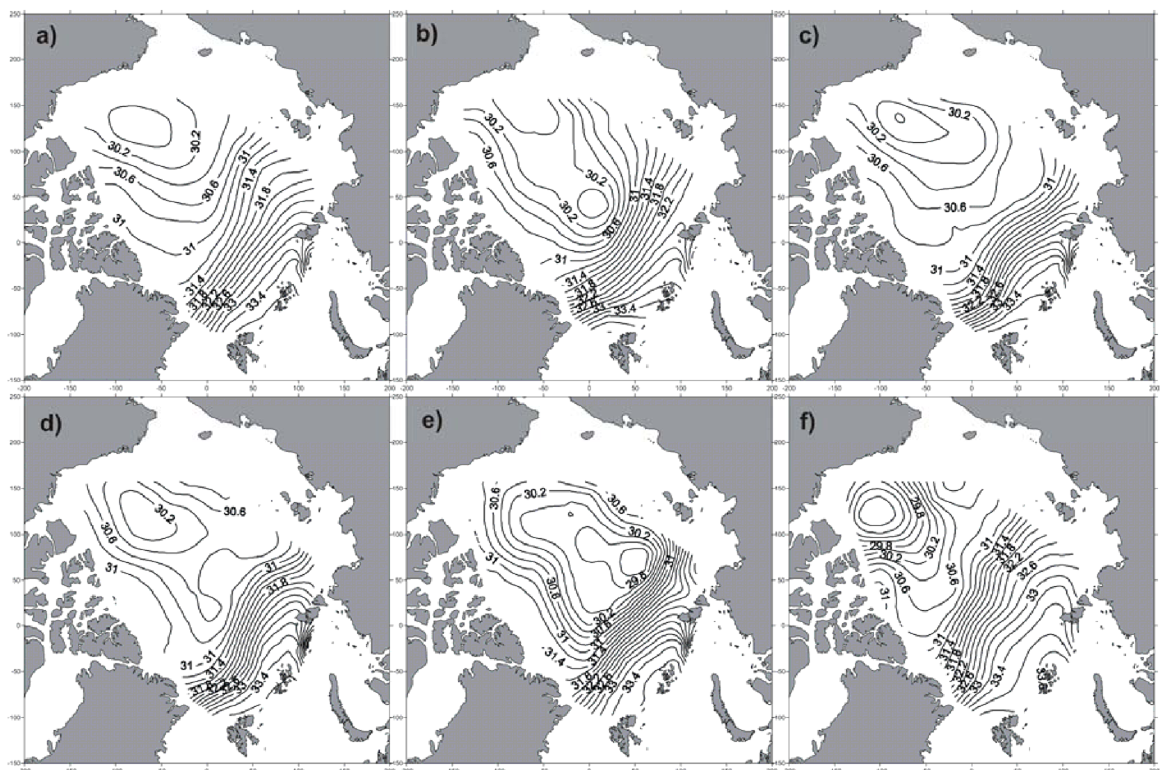

Fig. 3. Winter salinity fields for the layer 5-50 m averaged over periods to clusters: a – the cluster 1; b – the cluster 2; c – the cluster 3; d – the cluster 4; e – the cluster 5; f – the cluster 6.

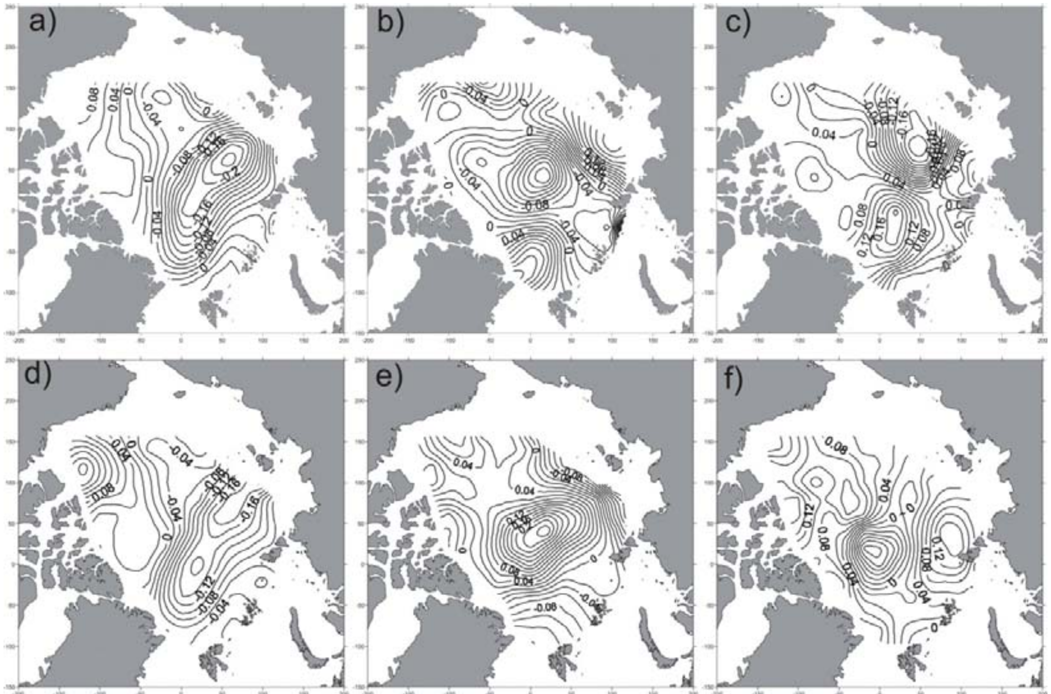

Fig. 4. The first three modes of the average salinity field decomposition for the layer 5-50 m: a, b, c - 1st, 2nd and 3rd modes, respectively, for the period 1950-1993.; d, e, f - 1st, 2nd and 3rd modes, respectively, for the period 1950-1993 and 2007-2011.

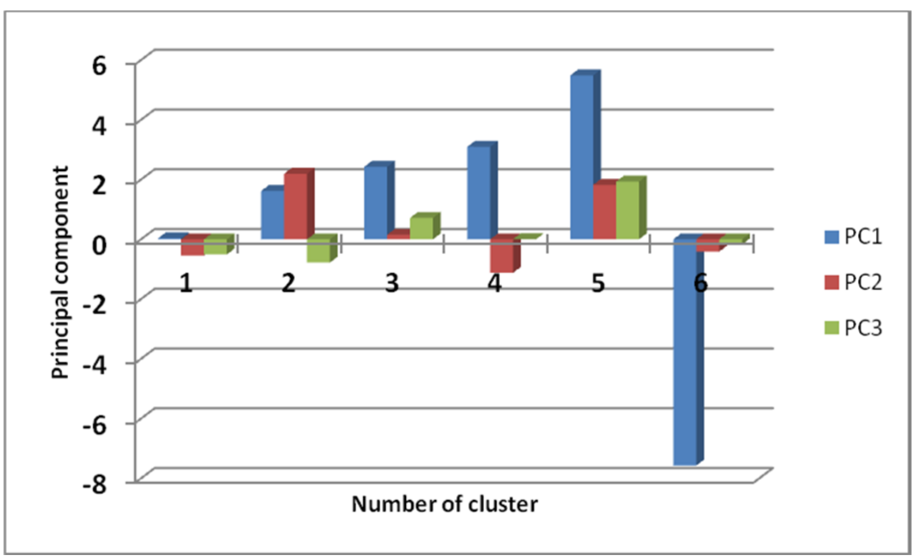

Fig. 5. The mean values of PCs for six clusters: 1 - 1950-59, 1976-77 and 1989; 2 - 1960-1965.; 3 – 1966-1975; 4 – 1981-1988; 5 – 1978-1980.; 6 – 1990-93 and 2007-2012.

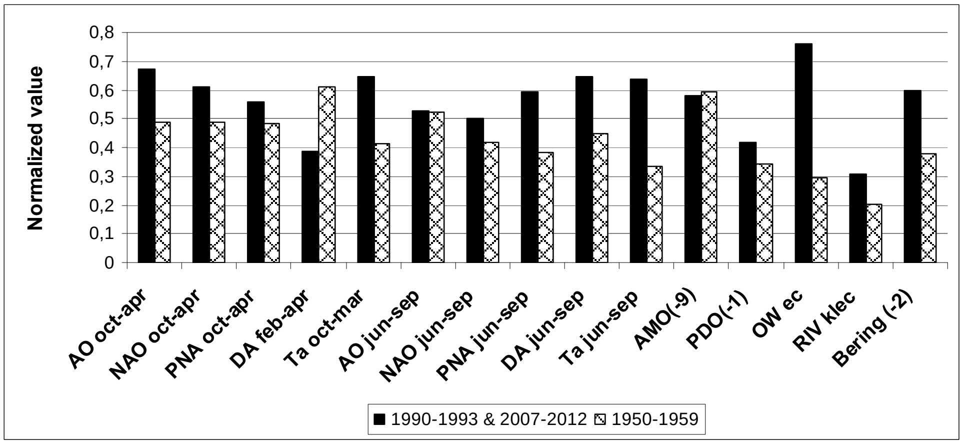

Figure 6. Mean values of the normalized values of the atmospheric circulation indexes (AO, NAO, PNA, DA, AMO, PDO); air temperature anomalies (Ta); areas of ice-free surface in the East Siberian and Chukchi Seas in September; river runoffs in the Kara, Laptev, East Siberian and Chukchi seas, the flow through the Bering Strait. Indexes of atmospheric circulation and temperature anomalies which averaged over the winter and summer months have been used in the calculations.

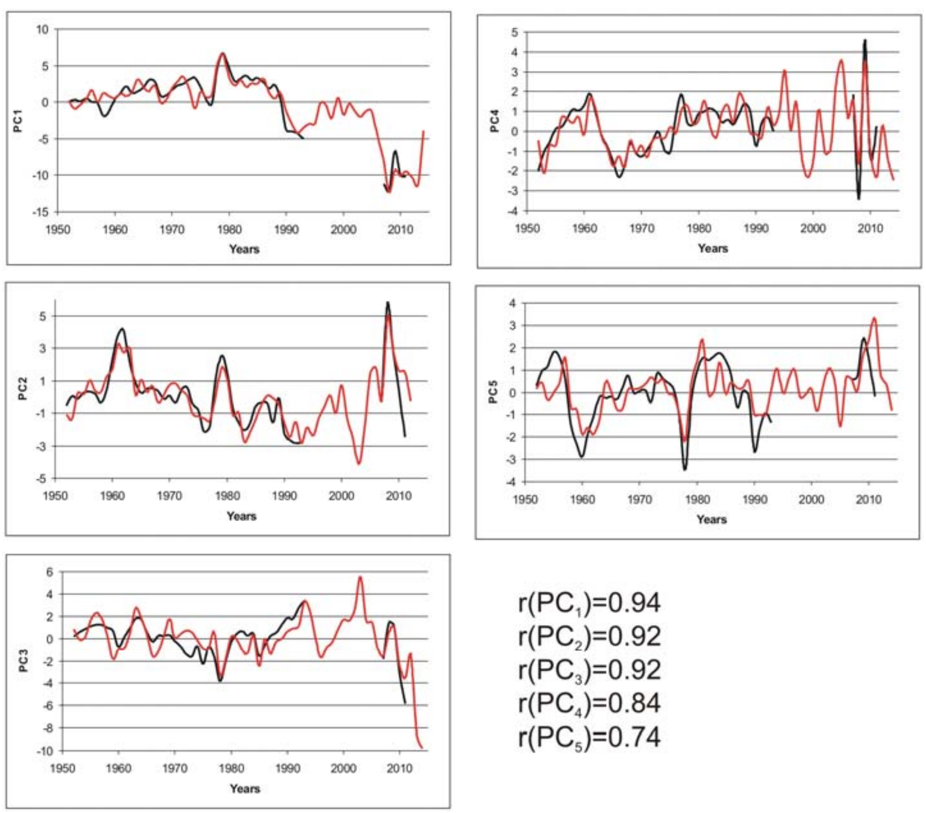

Figure 7. The real (black line) principal components and calculated principal components (red line) with help of the equations of linear regression. Also, we show the correlation coefficients between calculated time series of PC and the real PC, obtained by the decomposition of the salinity fields on EOF.

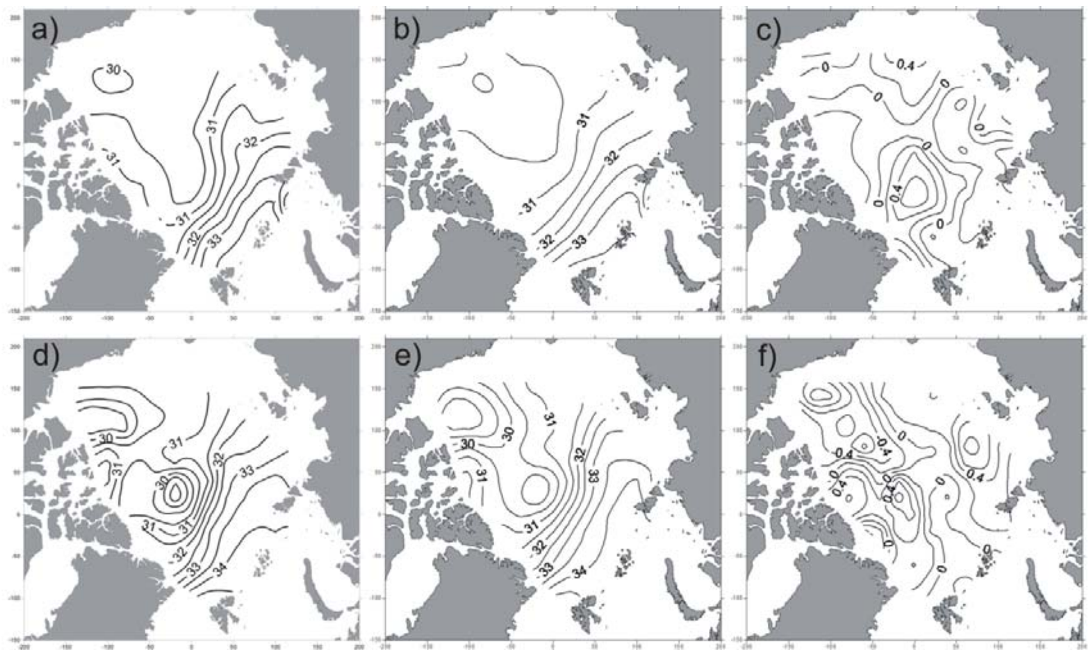

Figure 8. The real average salinity field for the layer of 5-50 m (a, d), the reconstructed average salinity field for the layer of 5-50 m (b, e) and the difference between of these fields (c, f) for 1955 (upper line) and 2009 (bottom line).

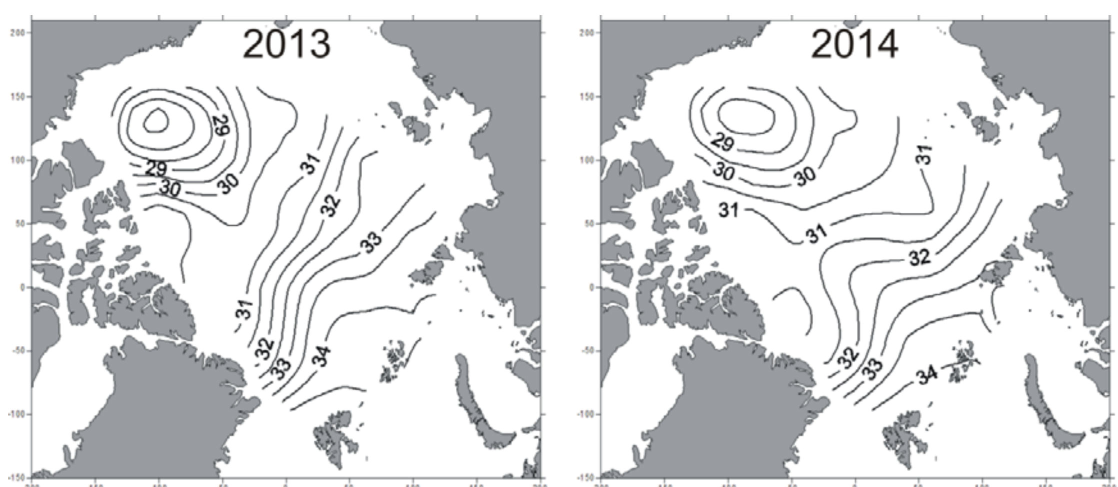

Figure 9. There is reconstructed salinity field for the layer of 5-50 m in 2013 and 2014.

Table 1. Predictors used for the approximation of PC.

Physical processes	Physical value	Description
Arctic oscillation index (AO)	sea-level pressure anomaly north of 20N latitude	When the AO index is positive, surface pressure is low in the polar region. When the AO index is negative, there tends to be high pressure in the polar region.
North Atlantic oscillation index (NAO)	sea-level pressure anomaly between the Icelandic low and the Azores high	When the NAO index is positive, pressures in the Azores high are especially high and pressures in the Icelandic low are lower than normal. Both pressure systems are located to the north. When the NAO index is negative, the Azores high and the Icelandic low are much weaker. Pressure differences are therefore smaller and both systems are located to the south.
Pacific/North American index (PNA)	sea-level pressure anomaly in the Northern Hemisphere extratropics	When the PNA index is positive, above-average heights over the Hawaii and over the intermountain region of North America, and below-average heights located south of the Aleutian Islands and over the southeastern United States. When the PNA index is negative, strong and extensive Hawaii high and a weak and very local Aleutian low are observed.
Arctic Dipole	sea-level	When the DA index is positive, sea-level pressure

Anomaly index (DA)	pressure anomaly north of 20N latitude	has positive anomaly over the Canadian Archipelago and negative anomaly over the Barents Sea. When the DA index is negative, SLP anomalies show an opposite scenario, with the center of negative SLP anomalies over the Nordic seas. (Wu et al, 2006; Wang et al, 2009; Overland & Wang, 2010)
Atlantic Multidecadal oscillation index (AMO)	Variations of sea surface temperature in the North Atlantic Ocean	Index has cool and warm phases that may last for 20-40 years at a time and a difference of about 0.5˚C. It reflects changes of sea surface temperature in Atlantic Ocean between the equator and Greenland. Was used as substitute for processes of water exchange with Atlantic Ocean.
The Pacific Decadal Oscillation index (PDO)	North Pacific sea surface temperature variability	When the PDO index is positive, the west Pacific becomes cool and part of the eastern ocean warms. When the DA index is negative, the opposite pattern occurs. It shifts phases on at least inter-decadal time scale, usually about 20 to 30 years.
Air temperature anomaly	degree	Monthly mean anomalies of air temperature over the Arctic
river runoff	water flows	Average annual runoff of the main Siberian rivers. Was used as total runoff in Kara Sea, Laptev Sea, East-Siberian Sea and Chukchi Sea.
Ice extent	area	Total ice extent in the Arctic Ocean in September

Area of open water in Arctic seas (OW)	area	Total ice-free area in Kara Sea, Laptev Sea, East-Siberian Sea and Chukchi Sea in September
Bering Strait inflow (BS)	water flows	Average annual water exchange through the Bering Strait